Journal of the Serbian Chemical Society
JSCS-info@shd.org.rs • www.shd.org.rs/JSCS
J. Serb. Chem. Soc. *75* (9) 1219–1230 (2010)
JSCS–4045
UDC 542.913:547.466+546.742:548.7:
541.121:536.7:535.33
Original scientific paper

Synthesis, crystal structure of and DFT calculations on bisglycinato-bis[*p*-(hydroxymethyl)pyridine]nickel(II)

PU SU ZHAO[1]*, JIE SONG[1], RONG CHANG SHANGGUAN[1] and FANG FANG JIAN[2]

[1]*Jiangsu Key Laboratory for Chemistry of Low-Dimensional Materials, Huaiyin Normal University, Huaian, Jiangsu, 223300 and* [2]*New Materials and Function Coordination Chemistry Laboratory, Qingdao University of Science and Technology, Qingdao Shandong, 266042, P. R. China*

(Received 28 October 2009, revised 12 January 2010)

Abstract: A new Ni(II) complex of bisglycinato-bis[*p*-(hydroxylmethyl)pyridine] was synthesized and characterized by elemental analysis, IR, UV–Vis spectroscopy and X-ray single crystal diffraction analysis. The thermal stability of the title complex was also determined. The complex adopts a distorted octahedral geometry and possesses inversion symmetry with the Ni(II) ion as the center of inversion. Density function theory (DFT) calculations of the structure, electronic absorption spectra, electron structure and natural population analysis (NPA) at the B3LYP/LANL2DZ level of theory were performed. The predicted geometric parameters and electronic spectra were compared with the experimental values and they supported each other. The NPA results indicate that the electronic transitions were mainly derived from the contribution of an intra-ligand (IL) transition, a ligand-to-metal charge transfer (LMCT) transition and a d-d transition. The electron structure calculations suggest that the central Ni(II) ion uses its 4s and 3d orbitals to form covalent bonds with coordinated N and O atoms. The calculated bond orders are also consistent with the thermal decomposition results. Based on vibrational analysis, the thermodynamic properties of the title complex were predicted and the correlative equations between these thermodynamic properties and temperature are also reported.

Keywords: amino acid complex; crystal structure; electronic spectra; DFT calculation; thermal stability.

INTRODUCTION

Recently, there is increasing interest in the realization of small and robust artificial DNA hydrolytic agents for their potential applications not only in molecular biology, but also in the development of new drugs.[1–3] Within these artificial nucleases, several examples of synthetic systems based on amino acid metal

* Corresponding author. E-mail: zhaopusu@163.com
doi: 10.2298/JSC091028101Z

complexes, which promote the hydrolysis of nucleic acids or of model phosphate esters, have been reported.[4–6] When the artificial nucleases establish interactions with DNA, metals are able to interact (covalently or not) with DNA through the electron-donating DNA bases and phosphate groups, thereby establishing either inter- or intra-strand interactions, while the coordinated groups in metal complexes contribute specific abilities, *i.e.*, intercalation, hydrogen bonding, electrostatic interaction, leading to a global effect.[1,7] On the other hand, nickel is an important trace element in organisms, which could promote the absorption of iron, the growth of erythrocyte and the synthesis of amino-enzyme in the body. It may also be a structural stabilizing agent of DNA and RNA.[8] Generally speaking, the Ni(II) ion frequently adopts coordination numbers of 4 or 6[9] and the coordination mode of Ni(II) depends on the structure of ligand, solvent and reaction conditions. Among these, the ligand plays a decisive role and determines not only the molecular structure of the complex, but also the aggregation fashion of the coordinated supermolecule.[10,11] Herein, a new Ni(II) complex with the amino acid bisglycinato-bis[*p*-(hydroxylmethyl)pyridine], in which the glycine exists as a bidentate chelating ligand and the complex adopts a distorted octahedral geometry, is reported. Density function theory (DFT) calculation results for the complex are also reported and compared with the experimental data. It is hoped that this report will provide useful structural information for the further study of the title compound with DNA.

EXPERIMENTAL

Physical measurements

Elemental analyses for carbon, hydrogen and nitrogen were performed by a Perkin-Elmer 240C elemental analyzer. The electronic absorption spectra were recorded on a Shimadzu UV3100 spectrophotometer in acetonitrile solution. Thermal gravimetric (TG) analysis was realized on an SDTA851e instrument (Mettler Toledo AG, Columbus, OH, USA) using samples of *ca* 10 mg under nitrogen (150 mL min^{-1}) at a heating rate of 20 °C min^{-1}.

Synthesis

All chemicals were obtained from a commercial source and used without further purification.

Freshly synthesized $Ni(OH)_2$ (0.93 g, 10 mmol), *p*-(hydroxymethyl)pyridine (2.18 g, 20.0 mmol) and glycine (1.5 g, 20 mmol) were mixed in water (50 mL) under stirring and the mixture was refluxed for 2 h. The resulting dark green solution was filtered and the filtrate was evaporated at room temperature. A dark green solid appeared which was separated by filtration. Yield: 68.2 % (2.9 g). Crystals suitable for X-ray structure determination were obtained by slowly evaporating an acetonitrile solution of the compound in air. Anal. Calcd. for $C_{16}H_{22}N_4NiO_6$: C, 45.20; H, 5.22; N, 13.18 %. Found: C, 45.14; H, 5.41; N, 13.01 %. IR (KBr, cm^{-1}): 3274(*s*), 2933 (*s*), 1586(*s*), 1499(*s*), 1393(*s*), 1350(*m*), 1302(*m*), 1225(*m*), 1130(*s*), 1057(*s*), 1017(*m*), 949(*m*), 898(*m*), 809(*m*), 722(*m*), 663(*m*), 590(*m*), 517(*m*).

Crystallographic data collection and solution of the structure

A summary of the key crystallographic information is given in Table I. The diffraction data were collected on an Enraf-Nonius CAD-4 diffractometer with graphite-monochromated Mo-Kα radiation (λ = 0.71073 Å, T = 293 K). The technique used was ω-scan with the limits 1.89 to 27.01°. The structure of the title compound was solved by direct methods and refined by least squares on F^2 using the SHELXTL[12] software package. All non-hydrogen atoms were anisotropically refined. The hydrogen atom positions were fixed geometrically at calculated distances and allowed to ride on the parent carbon atoms. The final conventional R = 0.0426 and Rw = 0.0906 for 1791 reflections with $I > 2\sigma(I)$ using the weighting scheme, w = = $1/(\sigma^2(F_0^2) + (0.0187P)^2 + 0.9868P$, where $P = (F_0^2 + 2F^{c2})/3$. The molecular graphics were plotted using SHELXTL software. Atomic scattering factors and anomalous dispersion corrections were taken from the International Tables for X-ray Crystallography.[13]

TABLE I. Summary of crystallographic results for the title compound

Empirical formula	$C_8H_{11}N_2Ni_{0.50}O_3$
Formula weight	212.54
Temperature, K	273(2)
Wavelength, Å	0.71073
Crystal system, space group	Monoclinic, *P*21/*c*
Unit cell dimensions, Å	a = 12.931(3)
	b = 5.6360(11), β = 123.35(2)°
	c = 14.476(6)
Volume, Å^3	881.3(5)
Z (calculated density, Mg/m^3)	4 (1.602)
Absorption coefficient, mm^{-1}	1.144
F(000)	444
θ range for data collection, °	1.89–27.01
Limiting indices	$-16 \le h \le 6$, $-7 \le k \le 7$, $-18 \le l \le 18$
Reflections collected/unique	3906/1837 (R_{int}= 0.0204)
Refinement method	Full-matrix least-squares on F^2
Data/restraints/parameters	1837/0/132
Goodness-of-fit on F^2	1.271
Final R indices ($I>2\sigma$ (I))	R_1 = 0.0426, wR_2 =0.0906
R indices (all data)	R_1 = 0.0439, wR_2 = 0.0912
Largest diffraction peak and hole, Å^{-3}	0.312 and –0.324

Computational methods

The initial molecular geometry was optimized using MM+ molecular modeling and semi-empirical AM1 methods (HYPERCHEM 6.0, Hypercube, Ont., Canada).[14] Then, DFT calculations with a hybrid functional B3LYP at the basis set LANL2DZ were performed by the Berny method[15] with the Gaussian 03 software package.[16] The calculated vibrational frequencies ascertained that the structure was stable (no imaginary frequencies). Based on the optimized geometry and using time-dependent density functional theory (TD-DFT)[17-19] methods, the electronic spectra of the title compound were predicted. Natural population analyses (NPA)[20] were also performed based on the optimized geometry.

All calculations were performed on a Dell PE 2850 server and a Pentium IV computer using the default convergence criteria.

RESULTS AND DISCUSSION

Crystal structure of the title compound

A displacement ellipsoid plot with the numbering scheme for the title compound is shown in Fig. 1. A perspective view of the crystal packing in the unit cell is shown in Fig. 2. Selected bond lengths and bond angles obtained by X-ray analysis are listed in Table II, together with the calculated bond parameters.

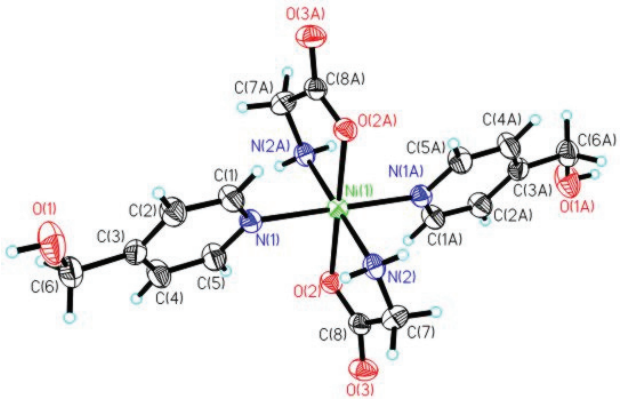

Fig. 1. Molecular structure of the title compound with atomic numbering.

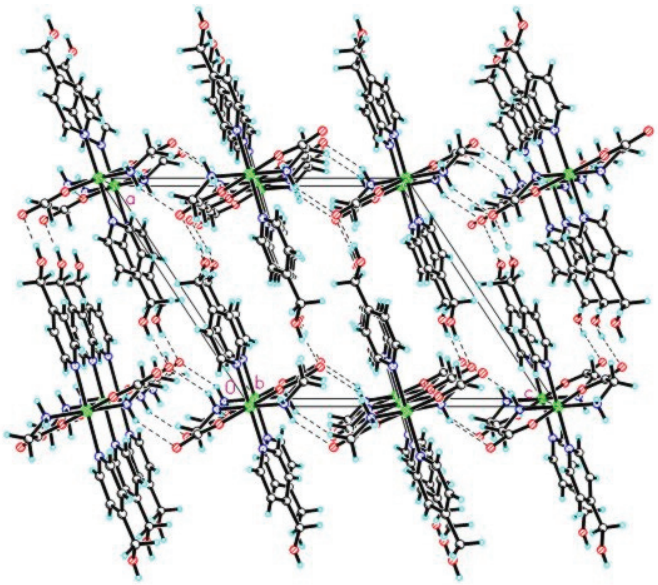

Fig. 2. Packing diagram of the unit cell along the *b*-axial direction for the title compound.

The crystal structure of the title complex is composed of two discrete monomeric molecules of $[(C_5H_4NCH_2OH)_2(CH_2NH_2COO)_2Ni(II)]$. The central nick-

el(II) ion is coordinated by two glycinato anions and two *p*-(hydroxymethyl)pyridine ligands with the Ni(II) ion as the center of inversion. The NiN_4O_2 core has a distorted octahedral geometry. The basal plane is formed by two oxygen atoms and two nitrogen atoms from the two glycinato anions and the chelating angle of N(1)–Ni(1)–O(2) is 81.08(9)°. The axial sites are occupied by two nitrogen atoms of the pyridyl rings from the two *p*-(hydroxymethyl)pyridine ligands. The bond length of Ni(1)–N(1) (2.162(2) Å) is slightly longer than that of Ni(1)–N(2) (2.075(2)Å), with both corresponding to those in other six-coordinated nickel(II) complexes.[21,22] The bond length of Ni(1)–O(2) is 2.063(19) Å, which is slightly longer than those in the above-cited structures (2.044(2) and 2.045(3) Å). All the bond lengths and bond angles in the *p*-(hydroxymethyl)pyridine ligand are within the normal range. The dihedral angle between the pyridine plane and the mean plane formed by atoms constituting the five-membered chelate ring is 86.72(1)°.

TABLE II. Selected geometric parameters from X-ray analysis and theoretical calculations at the B3LYP/LANL2DZ level of theory for the title compound

Bond length, Å					
Bond	Experimental	Calculated	Bond	Experimental	Calculated
Ni(1)–O(2)	2.063(19)	1.880	N(1)–C(1)	1.333(4)	1.356
Ni(1)–N(2)	2.075(2)	1.975	N(1)–C(5)	1.338(4)	1.356
Ni(1)–N(2A)	2.075(2)	1.975	N(2)–C(7)	1.471(4)	1.481
Ni(1)–N(1A)	2.162(2)	1.951	C(1)–C(2)	1.386(4)	1.398
Ni(1)–N(1)	2.162(2)	1.951	C(3)–C(4)	1.383(4)	1.408
O(1)–C(6)	1.402(4)	1.455	C(3)–C(6)	1.498(4)	1.514
O(2)–C(8)	1.263(3)	1.362	C(4)–C(5)	1.371(4)	1.401
O(3)–C(8)	1.249(3)	1.245	C(7)–C(8)	1.519(4)	1.539
Bond angle, °					
Bonds	Experimental	Calculated	Bonds	Experimental	Calculated
O(2)–Ni(1)–N(2)	81.08(9)	86.61	C(1)–N(1)–C(5)	116.4(2)	120.34
O(2A)–Ni(1)–N(2)	98.92(9)	93.39	N(1)–C(1)–C(2)	123.6(3)	120.95
O(2)–Ni(1)–N(2A)	98.92(9)	93.39	C(3)–C(2)–C(1)	119.5(3)	119.79
O(2A)–Ni(1)–N(2A)	81.08(9)	86.61	C(2)–C(3)–C(6)	122.9(3)	120.35
O(2)–Ni(1)–N(1)	90.96(8)	89.22	C(5)–C(4)–C(3)	119.9(3)	119.38
N(2)–Ni(1)–N(1)	89.73(9)	88.04	O(1)–C(6)–C(3)	110.6(3)	108.48
N(2A)–Ni(1)–N(1)	90.27(9)	91.96	N(2)–C(7)–C(8)	111.5(2)	110.00
C(8)–O(2)–Ni(1)	114.66(18)	115.68	O(2)–C(8)–C(7)	117.9(2)	113.79

In the crystal lattice, there are three types of hydrogen bonds and some weak intermolecular interactions (C–H···Y, Y = O)[23,24] (see Table III), which enable the molecules to form three-dimensional (3D) networks and stabilize the crystal structure.

TABLE III. Intermolecular hydrogen bonds and C–H···O supramolecular interactions

D–H···A	Symmetry on A	D···A Length, Å	∠D–H···A Angle, °
N(2)–H(1)···O(2)	*x*, 1+*y*, *z*	3.0633	167.42
O(1)–H(1A)···O(3)	1+*x*, 1/2–*y*, 1/2+*z*	2.7312	161.99
N(2)–H(2)···O(3)	–*x*, 1/2+*y*, 1/2–*z*	3.0631	151.30
C(1)–H(1B)···O(2)	–*x*, 1–*y*, *1–z*	3.0879	116.96
C(2)–H(2B)···O(1)	–	2.7468	100.53
C(5)–H(5A)···O(2)	–	3.0562	116.61

Optimized geometry

The optimized geometry possesses inversion symmetry and the Ni(II) is the center of inversion. A comparison of the theoretical and experimental values in Table III shows that most of the optimized bond lengths are slightly longer than those in the crystal structure and that larger differences mainly occur on the Ni(II) ion. The largest difference in bond length is 0.211 Å for Ni(1)–N(1) and the largest difference in bond angle is 5.53° for the angles around the Ni(II) ion, such as the bond angles O(2)–Ni(1)–N(2) and O(2A)–Ni(1)–N(2). The reason may be that the theoretical calculations consider isolated molecules in gaseous phase at 0 K while the experimental results belong to molecules in the solid phase. In the crystal state, the close packing of all the molecules and the existence of a crystal field result in the geometric parameters of the molecules differing from those found by calculations. On the other hand, those intermolecular hydrogen bonds and C-H···O supramolecular interactions in the crystal lattice may also lead to some differences in the bond lengths and bond angles between the experimental and predicted values. In spite of these differences, the Ni(II) ion in the optimized geometry still adopts a distorted octahedral coordination geometry and *p*-(hydroxymethyl)pyridine groups of the molecule represent a good approximation with the crystal structure. Based on the optimized geometry and natural population analysis (NPA), the electronic spectrum and thermodynamic properties of the title compound were calculated.

Electronic absorption spectra and electronic structure

The electronic absorption spectrum of the title compound in acetonitrile solution exhibits four bands. The two sharp peaks at 210 and 253 nm are ascribed to intra-ligand transitions between the glycinato anions and the *p*-(hydroxymethyl)pyridine groups, while the broad peak from 360 to 385 nm is assigned to charge transfer transitions from the low-energy π* orbital of the ligand to the d orbitals of the nickel (II) ion (LMCT).[25] The fourth broad band in the range of 540–556 nm arises from d–d transitions of Ni(II), which may be taken as evidence for octahedral Ni(II) complexes.[25] The DT-DFT electronic spectra calculations show that there are also four electronic transition bands which correspond to the experimental data. The two sharp predicted peaks are at 210 nm

(oscillator strength: 0.3454) and 238 nm (oscillator strength: 0.2610), respectively, and the band at 238 nm is blue shifted compared with the experimental value of 253 nm. The third broad band falls in the range of 300 to 370 nm with the biggest oscillator strength being 0.0401 at 342 nm, which has some blue shifts comparing with the experimental values of 360–385 nm. The fourth peak is from 470 to 520 nm with the largest oscillator strength of 0.0575 at 513 nm. This peak is located in the visible light range and is also blue shifted compared with the experimental data of 550–700 nm. The experimental and calculated electronic absorption spectra are shown in Fig. 3. Detailed experimental electronic absorption spectral values and the TD-DFT calculated ones, together with the detailed electronic transition modes, are given in Table IV. The reasons for the discrepancy between the experimental values and theoretical predictions may be as follows: TD-DFT approach is based on the random-phase approximation (RPA) method,[26,27] which provides an alternative to the computationally demanding multirefrence configuration interaction methods in the study of excited states. The TD-DFT calculations do not evaluate the spin-orbit splitting; the values are averaged. Here, in this paper, the objective was to evaluate the electronic structure by direct electronic excitations. Only singlet–singlet transitions are considered in these quasi-relativistic calculations. In addition, the role of the solvent effect of acetonitrile solution is not included in the theoretical calculations. Natural population analyses indicate that the frontier molecular orbitals are main-

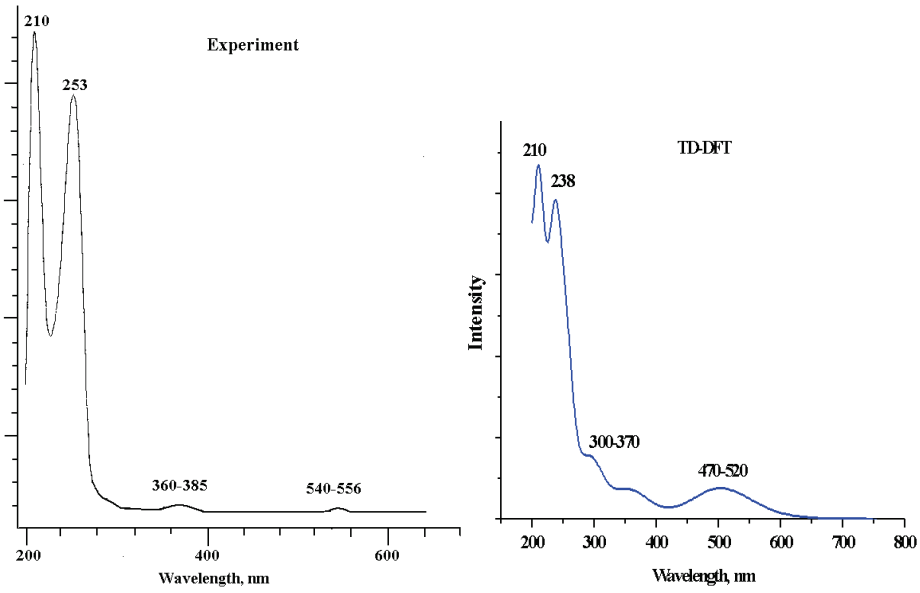

Fig. 3. Experimental (a) and calculated (b) electronic absorption spectra.

ly composed of d and p atomic orbitals, hence the above electronic transitions are mainly derived from the contribution of an intraligand (IL) transition, ligand-to-metal charge transfer (LMCT) transitions and d–d transitions. Some frontier molecular orbital stereographs for the title compound are shown in Fig. 4, from which it can be seen that the electron cloud distributions in the frontier molecular obitals support the above electronic transition models.

TABLE IV. Experimental and theoretical electronic absorption spectra values

Experimental		Calculated (TD-DFT)		
Wavelength, nm	Electronic transition modes	Wavelength, nm	Oscillator strength	Electronic transition modes
210	Intra-ligand	210	0.3454	104(HOMO-1) →108 (LUMO+2)
253	transition	238	0.2610	105(HOMO) →109 (LUMO+3)
360–385	LMCT	300–370	0.0401 at 342 nm	103 (HOMO-2) → →107 (LUMO+1)
540–556	d–d	470–520	0.0575at 513 nm	102 (HOMO-3) →106 (LUMO)

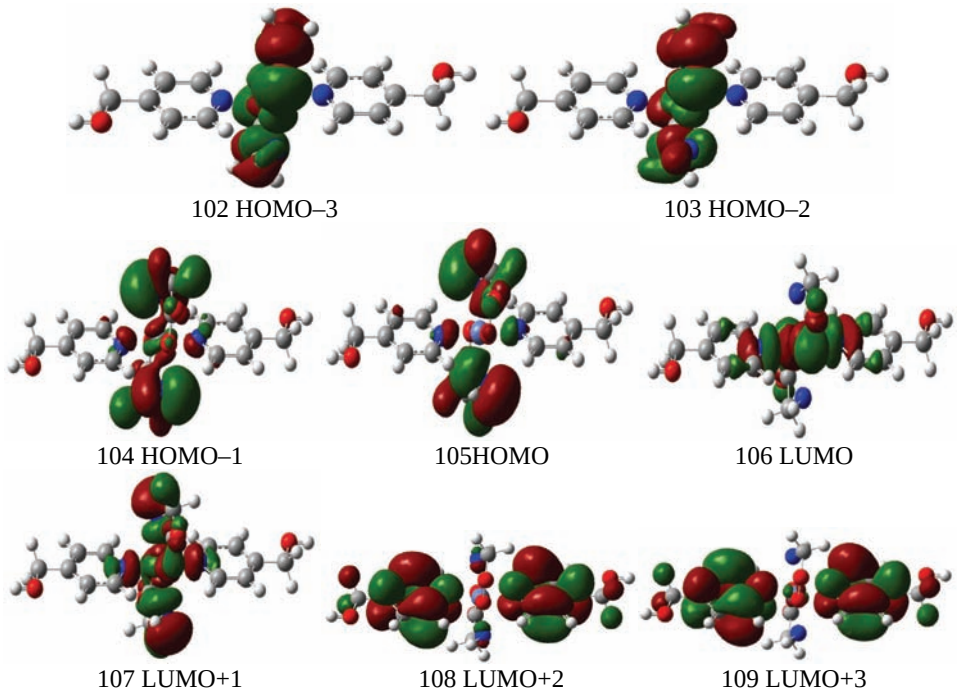

Fig. 4. Some frontier molecular orbital stereographs for the title compound.

The electronic structure of the title compound was calculated. The calculated natural population analysis charge and the natural electron configuration for the central Ni(1) ion and the coordinated N and O atoms are listed in Table V.

TABLE V. Natural population charge and natural electron configuration of the title compound

Atom	Net charge	Electron configuration
Ni(1)	1.22770	[core]4S(0.27)3d(8.46)4p(0.01)4d(0.01)5p(0.03)
N(1) and N(1A)	–0.48689	[core]2s(1.34)2p(4.12)3p(0.02)
N(2) and N(2A)	–0.87140	[core]2s(1.56)2p(4.29)3p(0.02)
O(2) and O(2A)	–0.73609	[core]2s(1.76)2p(4.96)3p(0.01)

From Table V, it can be seen that the net charge on the Ni(1) ion is +1.22770, deviating from +2. The net charges on the coordinated N atoms range from –0.48689 to –0.87140 and the net charges on the coordinated O atoms are both –0.73609, showing that these atoms transfer parts of their electrons to the central Ni(1) ion and then covalent bonds are formed. On the other hand, from the natural electron configuration, for the Ni(1) ion, the electron number of 4s (0.27) is larger than zero, the electron number of 3d (8.26) is larger than 8 and those of 4p, 4d and 5p are so small that can be neglected. These data suggest that the Ni(1) ion uses its 4s and 3d orbitals to form covalent bonds with the N and O atoms. While for the coordinated N and O atoms, the electron number of the 2s orbital ranges from 1.34 to 1.76 and can be ascribed to lone pair electrons.[28] The 2p orbital falls in the range of 4.12–4.96. Thus, it can be concluded that the coordinated N and O atoms form covalent bonds with the Ni(1) ion having 2p orbitals.

Thermal property analysis and the bond order

The thermal gravimetric curve of the title compound is given in Fig. 5, from which it can be seen that the decomposition of the title compound is accompanied by two mass-loss processes, the first one from 220 to 280 °C and the second one from 300 to 420 °C. During the first weight-loss process, the mass loss is 49.96 %, which can be assigned to the breakage of the Ni(1)–N(1) and Ni(1)–N(1A) bonds and the decomposition of the *p*-(hydroxymethyl)pyridine groups (Calcd. 51.35 %). After 300 °C, the second decomposition step accompanied by a weight loss of 34.62 % occurs, which is assigned to the scission of the Ni(1)–O(2), Ni(1)–N(2), Ni(1)–O(2A) and Ni(1)–N(2A) bonds and the loss of two glycinato anions (Calcd. 34.84 %). The residue of the decomposition (15.42 %) is Ni (Calcd. 13.81 %). These experimental facts reveal that the Ni(1)–N(1) and Ni(1)–N(1A) bonds are weaker than the Ni(1)–O(2), Ni(1)–O(2A), Ni(1)–N(2) and Ni(1)–N(2A) bonds. Theoretical calculations at the B3LYP/LANL2DZ level of theory show that the bond orders of the Ni(1)–N(1) and Ni(1)–N(1A) bonds are both 0.0973. The bond orders of the Ni(1)–O(2) and Ni(1)–O(2A) bonds are both 0.2770 and the bond orders of the Ni(1)–N(2) and Ni(1)–N(2A) bonds are both 0.3692. It is obvious that thermal analysis of the title compound proved the theoretical predictions to be correct. In other words, the theoretical calculations support the experimental facts.

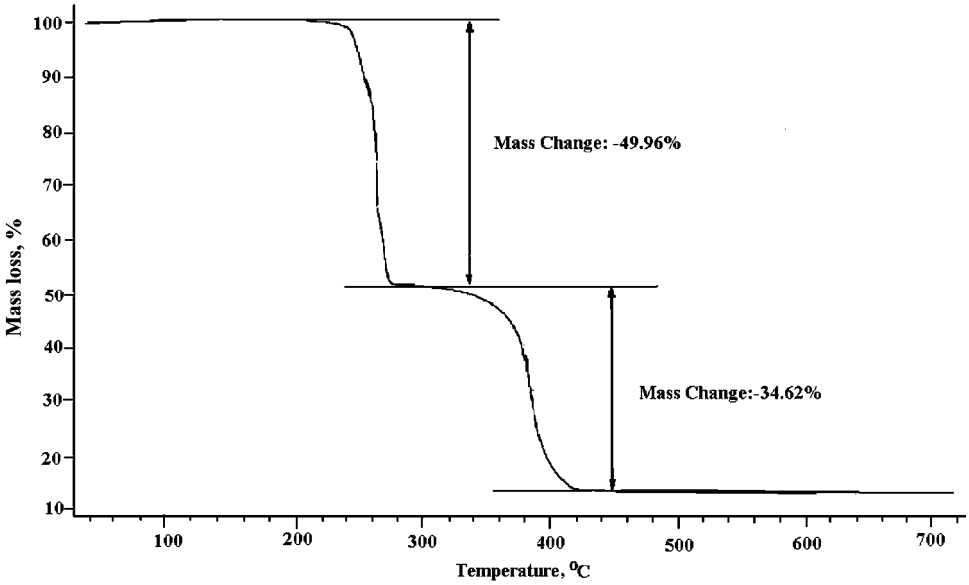

Fig. 5. Thermal gravimetric curve of the title compound.

Thermodynamic properties

Based on vibrational analysis at the B3LYP/LANL2DZ level and statistical thermodynamics, the standard thermodynamic functions: heat capacities ($C^0_{p,m}$), entropies (S^0_m) and enthalpies (H^0_m), were obtained and are listed in Table VI. The scale factor for frequencies is 0.96, which is a typical value for the B3LYP method.

TABLE VI. Thermodynamic properties of the title compound at different temperatures at the B3LYP/LANL2DZ level

T / K	$C^0_{p,m}$ / J·mol^{-1}·K^{-1}	S^0_m / J·mol^{-1}·K^{-1}	H^0_m / kJ·mol^{-1}
200.0	320.0	620.1	37.27
300.0	444.3	773.5	75.51
400.0	558.0	917.3	125.8
500.0	651.9	1052	186.4
600.0	726.6	1178	255.5
700.0	786.2	1295	331.3
800.0	834.6	1403	412.4

From Table VI, it can be observed that the standard heat capacities, entropies and enthalpies increase at any temperature ranging from 200.0 to 800.0 K because the intensities of molecular vibration increase with increasing temperature.

The correlative equations between these thermodynamic properties and temperatures are as follows:

$$C^0_{p,m} = 17.407 + 1.675T - 8.196\times10^{-4}T^2,\ R^2 = 0.9999$$
$$S^0_m = 287.124 + 1.756T - 4.521\times10^{-4}T^2,\ R^2 = 0.99999$$
$$H^0_m = -22.348 + 0.204T + 4.270\times10^{-4}T^2,\ R^2 = 0.9998$$

These equations will be helpful for the further studies of the title compound. For instance, when the interaction between the title compound and another compound is investigated, the thermodynamic properties $C^0_{p,m}$, H^0_m and S^0_m could be obtained from these equations and then used to calculate the change of Gibbs free energy of the reaction, which will assist in the judgement of the spontaneity of the reaction.

Supplementary material. CCDC – 649102 contains the supplementary crystallographic data for this paper. These data can be obtained free of charge at http://www.ccdc.cam.ac.uk/conts/retrieving.html or from the Cambridge Crystallographic Data Centre (CCDC), 12 Union Road, Cambridge CB2 1EZ, UK (fax: +44(0)1222-336033; e-mail: deposit@ccdc.cam.ac.uk).

Acknowledgement. This work was supported by Jiangsu Key Laboratory for Chemistry of Low-Dimensional Materials P. R. China (JSKC08047) and Fund of Huanyin Normal University (08HSJSK003).

ИЗВОД

СИНТЕЗА, КРИСТАЛНА СТРУКТУРА И DFT ИЗРАЧУНАВАЊА ЗА БИСГЛИЦИНАТО--БИС[*p*-(ХИДРОКСИМЕТИЛ)ПИРИДИН]-НИКАЛ(II)

PU SU ZHAO[1], JIE SONG[1], RONG CHANG SHANGGUAN[1] и FANG FANG JIAN[2]

[1]*Jiangsu Key Laboratory for Chemistry of Low-Dimensional Materials, Huaiyin Normal University, Huaian, Jiangsu, 223300 и* [2]*New Materials and Function Coordination Chemistry Laboratory, Qingdao University of Science and Technology, Qingdao Shandong, 266042, P. R. China*

Синтетозован је нови бисглицинато-бис[*p*-(хидроксиметил)пиридин]-никал(II) комплекс. Поред елементарне микроанализе, за карактеризацију овог комплекса употребљени су IR и UV–Vis спектри, као и кристална дифракциона анализа помоћу X-зрака. Одређена је термичка стабилност добивеног комплекса. Нађено је да комплекс има дисторговану октаедраску геометрију и инверзиону осу симетрије са Ni(II) јоном у центру инверзије. Структура комплекса потврђена је на основу теоријских израчунавања применом методе функционалних густина (DFT израчунавања), електронских апсорпционих спектара, електронске структуре и NPA анализе за B3LYP/LANL2DZ теоријски степен. Предвиђени геометријски параметри и електронски спектри су у сагласности са одговарајућим експерименталним вредностима. Добијени NPA параметри указују да електронски прелази углавном деривирају од доприноса интралигандних (IL) прелаза, прелаза који потичу од лиганд-метал трансфера наелектрисања (LMCT) и d–d прелаза. Израчунавања електронске структуре указују да централни Ni(II) јон користи 4s и 3d орбитале за грађење ковалентних веза са донорским N и O атомиима. Израчунате вредности дужина веза су такође, у сагласности са резултатима добивеним на основу термичке декомпозиције комплекса. На основу вибрационих анализа предвиђене су термодинамичке особине добивеног Ni(II) комплекса и дате су корелативне једначине које повезују ове термодинамичке особине са температуром.

(Примљено 28. октобра 2009, ревидирано 12. јануара 2010)

REFERENCES

1. M. Livieri, F. Mancin, U. Tonellato, J. Chin, *Chem. Commun*. **24** (2004) 2862
2. L. Fernandes, F. L. Fischer, C. W. Ribeiro, G. P. Silveira, M. M. Sá, F. Nome, H. Terenzi, *Bioorg. Med. Chem. Lett.* **18** (2008) 4499
3. X. Q. Chen, J. Y. Wang, S. G. Sun, J. L. Fan, S. Wu, J. F. Liu, S. J. Ma, L. Z. Zhang, X. J. Peng, *Bioorg. Med. Chem. Lett.* **18** (2008) 109
4. P. U. Maheswari, S. Roy, H. den Dulk, S. Barends, G. van Wezel, B. Kozlevöar, P. Gamez, J. Reedijk, *J. Am. Chem. Soc*. **128** (2006) 710
5. S. Negi, Y. Umeda, S.Masuyama, K. Kano, Y. Sugiura, *Bioorg. Med. Chem. Lett.* **19** (2009) 2789
6. M. Dhanasekaran, S. Negi, Y. Sugiura, *Acc. Chem. Res*. **39** (2006) 45
7. L. Otero, P. Smircich, M. Vieites, M. Ciganda, P. C. Severino, H. Terenzi, H. Cerecetto, D. Gambino, B. Garat, *J. Inorg. Biochem.* **101** (2007) 74
8. J. G. Yang, F. Li, F. Y. Pan, W. P. Jia, *Chin. J. Struct. Chem.* **26** (2007) 1071
9. B. Gillon, C. Mathoniere, E. Ruiz, S. Alvarez, A. Cousson, T.M. Rajendiran, O. Kahn, *J. Am. Chem. Soc*. **124** (2002) 14433
10. S. Noro, R. Kitaura, M. Kondo, S. Kitagawa, T. Ishii, H. Matsuzaka, M. Yamashita, *J. Am. Chem. Soc*. **124** (2002) 2568
11. M. Devereux, M. McCann, D. O. Shea, R. Kelly, D. Egan, C. Deegan, K. Kavanagh, Y. McKee, G. Finn, *J. Inorg. Biochem.* **98** (2004) 1023
12. G. M. Sheldrick, *SHELXTL, v. 5 Reference Manual*, Siemens Analytical X-Ray Systems, Madison, WI, 1997
13. A. J. Wilson, *International Table for X-Ray Crystallography*, Vol. C, Kluwer Academic, Dordrecht, 1992, pp. 500–502, 219–222
14. M. J. S. Dewar, E. G. Zoebisch, E. F. Healy, J. J. P. Stewart, *J. Am. Chem. Soc*. **107** (1985) 3902
15. C. Peng, P. Y. Ayala, H. B. Schlegel, M. J. Frisch, *J. Comput. Chem.* **17** (1996) 49
16. *Gaussian 03 software package*, Gaussian Inc., Wallingford, CT, 2004
17. E. Runge, E. K. U. Gross. *Phys. Rev. Lett.* **52** (1984) 997
18. M. Petersilka, U. J. Gossmann, E. K. U. Gross, *Phys. Rev. Lett.* **76** (1966) 1212
19. R. Bauernschmitt, R. Ahlrichs, *Chem. Phys. Lett.* **256** (1996) 454
20. C. Jamorski, M. E. Casida, D. R. Salahub. *J. Chem. Phys.* **104** (1996) 5134
21. B. F. Abrahams, B. F. Hoskins, T. A. Hudson, R. Robson, *Acta Crystallogr., Sect. C* **56** (2000) e126
22. M. Du, X. H. Bu, M. Shionoya, M. Shiro, *J. Mol. Struct.* **607** (2002) 155
23. T. Steiner. *Crystallogr. Rev.* **6** (1996) 1
24. G. A. Jeffrey, H. Maluszynska, J. Mitra, *Int. J. Biol. Macromol.* **7** (1985) 336
25. F. F. Jian, L. Pang, H. L. Xiao, P. P. Sun, *Chin. J. Struct. Chem.* **23** (2004) 975
26. L. Olsenand, P. Jorgensen. in: *Modern Electronic Structure Theory*, Vol. 2, World Science, River Edge, NJ, 1995
27. M. Fernando, O. Claudio, *Int. J. Quantum Chem.* **103** (2005) 34
28. H. H. Li, Z. R. Chen, J. Q. Li, C. C. Huang, B. Zhao, Z. X. Ni, *Chin. J. Struct. Chem.* **24** (2005) 39.